8-2004

Results from the Middle Atmosphere with the Rayleigh-Scatter Lidar at USU's Atmospheric Lidar Observatory

Vincent B. Wickwar
Utah State University

Joshua P. Herron
Utah State University

Troy A. Wynn

Eric M. Lundell

Results from the Middle Atmosphere with the Rayleigh-Scatter Lidar at USU's Atmospheric Lidar Observatory

Vincent B. Wickwar, Joshua P. Herron, Troy A. Wynn, and Eric M. Lundell
Utah State University / Center for Atmospheric and Space Sciences
Logan, UT 84322-4405

Atmospheric Regions

Atmospheric regions are characterized by their temperature gradient, dT/dz, a illustrated in **Figure 1**. Starting from the ground, there is the

- **Troposphere**—negative gradient
- **Stratosphere**—positive gradient
- **Mesosphere**—negative gradient
- **Thermosphere**—positive gradient

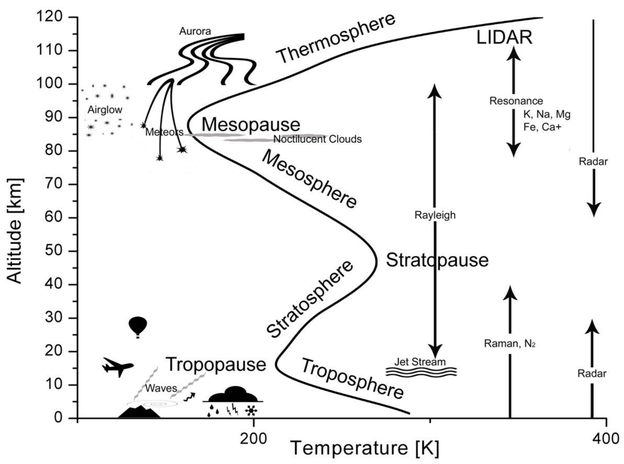

Figure 1. Atmospheric Regions. The middle atmosphere extends from 10 to 110 km. Most of the ALO observations are in the mesosphere.

The region 30–80 km (20–50 miles) was known as the ignorosphere for a long time because of the difficulty of making measurements:

- Balloons and planes only go to 30 km (20 miles)
- Optical emissions occur above 80 km (50 miles)
- Radio techniques have a gap from 30 to ~80 km
- Rockets work, but are expensive
- Satellites work, but do not provide a time history.

The development of the laser opened up research in this region. USU has been operating a Rayleigh-scatter lidar since 1993 to observe the region 45–90 km (28–56 miles). It is 1 of 6 such lidars in the world making regular observations.

Lidar

Lidar (**LI**ght **D**etection **a**nd **R**anging) is analogous to radar, except that it uses visible, or near visible, light instead of radio waves. **Figure 2** shows the lidar starting with a laser (**L**ight **A**mplification by **S**timulated **E**mission of **R**adiation), which is analogous to a transmitter. The ALO laser is a frequency-doubled, solid-state, Nd:YAG laser emitting 18 W in the green, **Figure 3**.

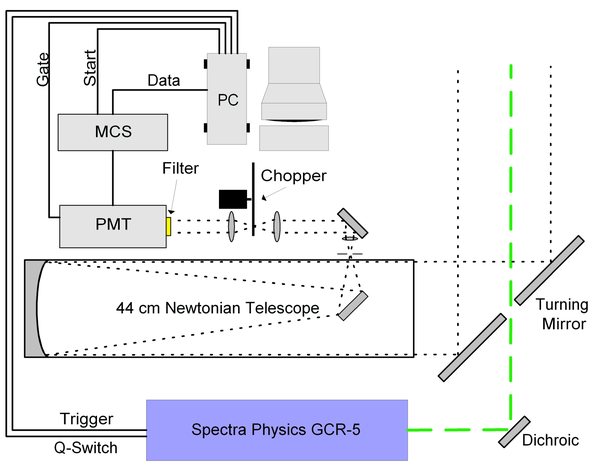

Figure 2. Schematic diagram of ALO lidar.

Each laser pulse lasts 7 ns (~7 feet long) and repeats at a 30 Hz rate. It appears continuous. At all altitudes, a very small portion of the light is Rayleigh scattered in all directions from gas molecules (mostly N_2 and O_2) and, at some altitudes, it is also Mie scattered from aerosols (e.g., dust, water droplets, ice crystals).

A telescope, analogous to a radar antenna or dish, is used to collect as much of the scattered light as possible. ALO's telescope is 44 cm (17 inches) in diameter. The detector is a photomultiplier tube (PMT), which puts out an electron pulse for each detected photon. A multichannel scaler (MCS) counts these pulses vs time. The altitude is determined by the speed of light and the round-trip time from when the pulse is emitted, e.g., 400 μs for 60 km (38 miles).

Figure 3. Green beam from ALO Rayleigh-scatter lidar.

These profiles provide the molecular number density for 30–100 km. At lower altitudes and, occasionally, near 83 km, these profiles are contaminated by scattering from aerosols. Absolute temperatures are then derived from these relative density profiles.

We will now show the 10-year density and temperature climatologies and two indications of global change.

Density Climatology

The relative densities are made absolute by normalizing to the MSISe00 empirical model at 45–48 km. The multiyear, annual, mean density $\langle D_{yr} \rangle$ is found by averaging the 12 multiyear, monthly mean densities $\langle D_{mn} \rangle$, **Figure 4**. It decreases by 10^4 by 100 km, reaching what would be a good vacuum in the laboratory. To show monthly variations, $[\langle D_{mn} \rangle - \langle D_{yr} \rangle]/\langle D_{yr} \rangle$, the fractional difference relative to $\langle D_{yr} \rangle$, is plotted vs altitude in **Figure 5**. The overall climatology is shown in **Figure 6**. The major annual variability, almost ±20%, occurs near 70 km with a summer maximum and winter minimum. Another minimum occurs at 90–95 km in summer.

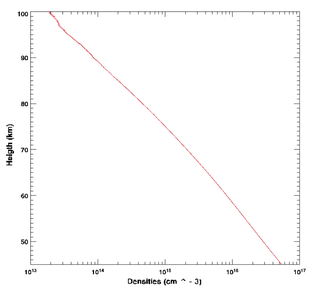

Figure 4. Multiyear, annual, mean density $\langle D_{yr} \rangle$ with uncertainties.

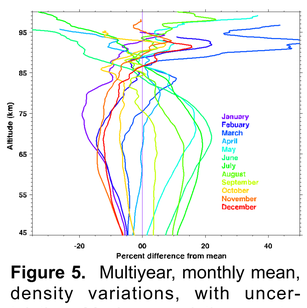

Figure 5. Multiyear, monthly mean, density variations, with uncertainties. Maximum variation, greater than ±20%, occurs near 70 km.

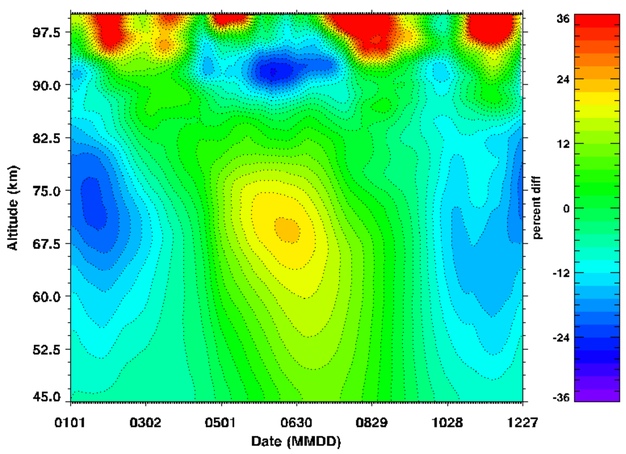

Figure 6. ALO density climatology. These densities have extra smoothing in altitude and time. Like Figure 5, this is valid up to approximately 95 km.

Temperature Climatology

Because the absolute temperatures vary over a much smaller range than the densities, they are shown instead of their variations. Each profile in **Figure 7** shows a multiyear, monthly mean temperature $\langle T_{mn} \rangle$. Near the stratopause, the temperatures are much hotter in summer than in winter because the heating is dominated by solar radiation. Near 85 km, the reverse occurs; the temperatures are much colder in summer than in winter! This happens because the heating is dominated by atmospheric dynamics instead of insolation. These curves cross near 62 km. This behavior makes the detailed physics of the mesosphere particularly interesting. These curves also show the mesopause near 85 km in summer, but indicate it is much higher in winter. They also show an almost permanent mesospheric temperature inversion layer near 65–75 km in December–March.

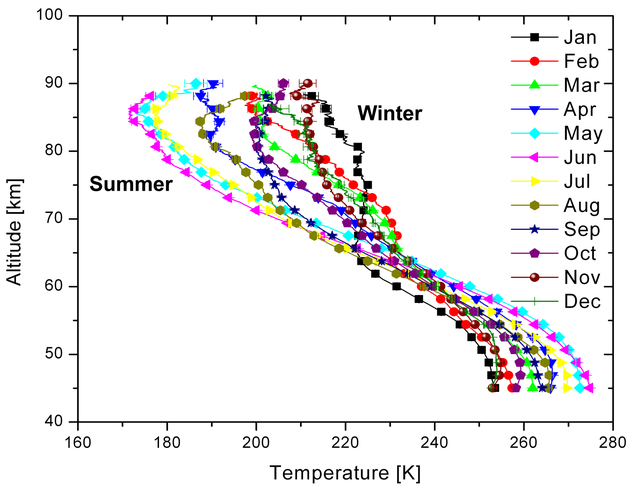

Figure 7. Multiyear, monthly mean, temperature profiles with uncertainties.

The full, detailed temperature climatology is shown in **Figure 8**. The basic average is over 31 days and 3 km. To emphasize the major features, additional smoothing has been carried out over 14 days and 1.5 km. In addition to the features described above, a significant spring-fall asymmetry appears along with significant warmings near spring and fall equinox at high altitudes.

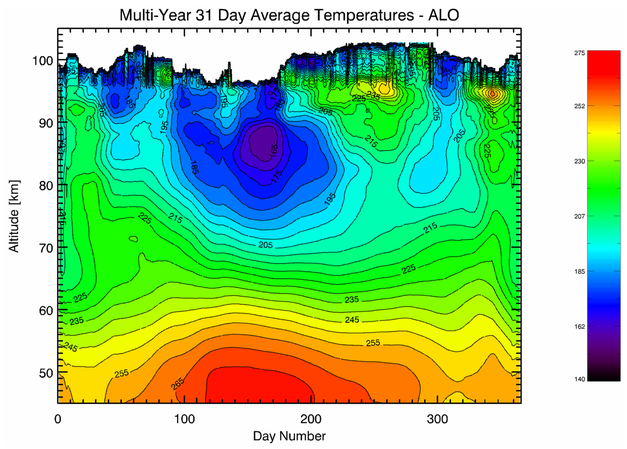

Figure 8. ALO temperature climatology. The temperatures are valid starting 5–10 km below the maximum altitude. The smoothing for the densities in Figure 6 is the same as for these temperatures.

Global Change

In addition to providing the density and temperature climatologies, the extensive ALO dataset provides information related to global change. This shows up in temperature trends and in the detection of noctilucent clouds (NLCs). While the build up of greenhouse gases, of which CO_2 is the most important, is expected to lead to tropospheric heating, model calculations indicate that it should lead to mesospheric cooling. The concept is that energy carried by upward infrared radiation from these gases will be lost to space, thereby acting like a refrigerator. (This leaves out other possible effects such as changes in the atmospheric circulation and the impact of tropospheric and stratospheric changes on the mesosphere.) A small linear temperature trend has been sought in the ALO data. It has to be separated from comparable and larger variations arising from the summer-winter cycle, episodic events such as volcanic eruptions, and the 11-year solar cycle. The results are shown by the solid red line in **Figure 9**. The dashed lines show the 95% confidence limits.

In addition to increases in greenhouse gases, there is a significant increase in methane CH_4. Through a combination of dissociation by solar radiation (photolysis), oxidation, and chemical reactions, this leads to an increase in water vapor in the upper mesosphere.

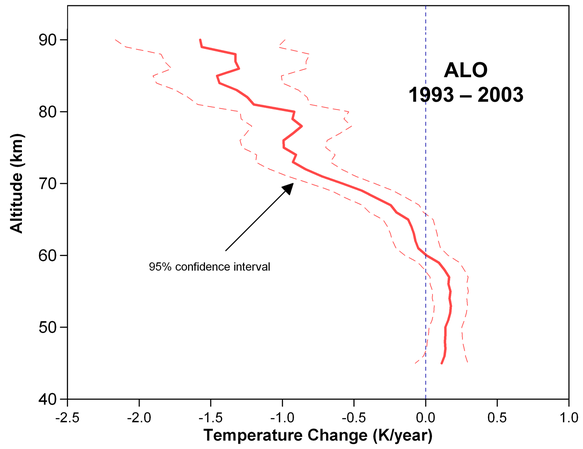

Figure 9. Linear temperature trend. This shows significant cooling of 10–15 K per decade in the upper mesosphere and, possibly, slight heating near the stratopause .

At latitudes greater than 50°, the cold summer temperatures, colder than above USU, and high water vapor densities give rise to NLCs, composed of ice crystals, near 83 km. Thus, it was very surprising when NLCs were detected above USU at 41.7°N latitude in June 1995 and June 1999. **Figure 10** shows the first of these clouds. What is shown is the backscatter ratio, which is 1.0 for Rayleigh scatter and greater than 1.0 for combined Rayleigh and Mie scatter.

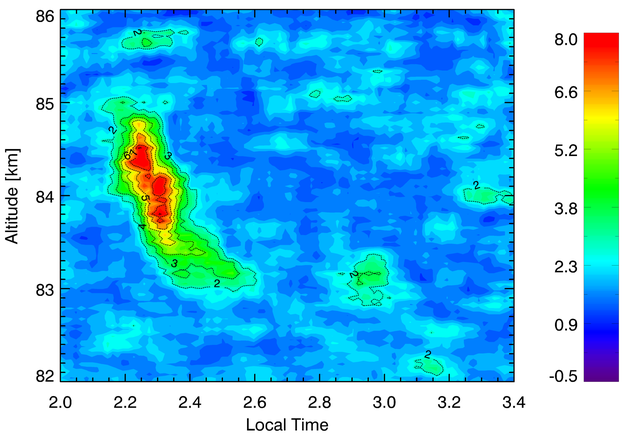

Figure 10. Backscatter ratio for 23 June 1995. Smoothing is over 150 m in altitude and 12 minutes in time. The NLC occurs between 83 and 85 km and between 2.2 and 2.6 local time and, perhaps, near 3.0 local time. The small patches with small backscatter ratios reflect the noise level of the data.

This simple global change implication is for lower temperatures and greater water vapor above USU. However, the 140 K temperature found in the vicinity of the cloud did not arise from uniform cooling. Instead, as shown in **Figure 11**, a large temperature wave reduced the temperature near 83 km ~20 K below the mean temperature. Thus, while the NLC appeared at lower latitudes as predicted by global change, the mechanism is more complicated than uniform mesospheric cooling. The large amplitude wave may be another aspect of global change.

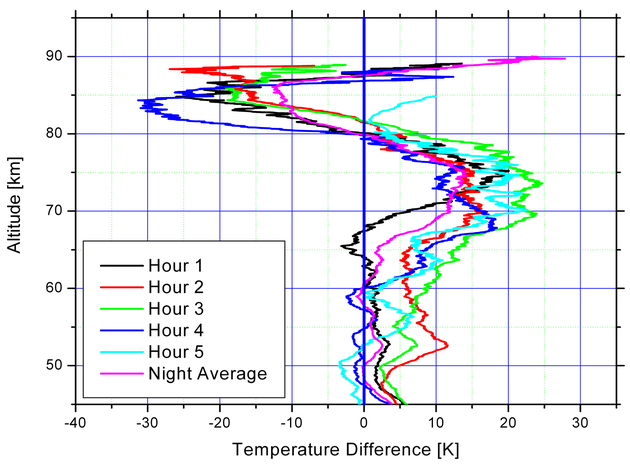

Figure 11. Differences between the observed temperatures on 23 June 1995 and the multiyear, 31-day averaged temperatures. The maximum for the negative phase of a large temperature wave is located near 83 km. The positive peak is approximately 10 km lower.

Acknowledgements: This work was partially supported by USU, the Rocky Mountain Space Consortium, and grants from the Atmospheric Sciences Division of the National Science Foundation. The authors also gratefully acknowledge the many undergraduates who spend long nights operating the lidar.

For additional information, contact vincent.wickwar@usu.edu.

August 2004